esa

ECOSPHERE

INNOVATIVE VIEWPOINTS

Ecohydrology with unmanned aerial vehicles

ENRIQUE R. VIVONI,[1,2,]† ALBERT RANGO,[3] CODY A. ANDERSON,[1] NICOLE A. PIERINI,[1] ADAM P. SCHREINER-MCGRAW,[2] SRIKANTH SARIPALLI,[2] AND ANDREA S. LALIBERTE[3]

[1]*School of Sustainable Engineering and the Built Environment, Arizona State University, Tempe, Arizona 85287 USA*
[2]*School of Earth and Space Exploration, Arizona State University, Tempe, Arizona 85287 USA*
[3]*United States Department of Agriculture, Agricultural Research Service, Jornada Experimental Range, 2995 Knox Street, Las Cruces, New Mexico 88003 USA*

Citation: Vivoni, E. R., A. Rango, C. A. Anderson, N. A. Pierini, A. P. Schreiner-McGraw, S. Saripalli, and A. S. Laliberte. 2014. Ecohydrology with unmanned aerial vehicles. Ecosphere 5(10):130. http://dx.doi.org/10.1890/ES14-00217.1

Abstract. High-resolution characterizations and predictions are a grand challenge for ecohydrology. Recent advances in flight control, robotics and miniaturized sensors using unmanned aerial vehicles (UAVs) provide an unprecedented opportunity for characterizing, monitoring and modeling ecohydrologic systems at high-resolution (<1 m) over a range of scales. *How can the ecologic and hydrologic communities most effectively use UAVs for advancing the state of the art?* This Innovative Viewpoints paper introduces the utility of two classes of UAVs for ecohydrologic investigations in two semiarid rangelands of the southwestern U.S. through two useful examples. We discuss the UAV deployments, the derived image, terrain and vegetation products and their usefulness for ecohydrologic studies at two different scales. Within a land-atmosphere interaction study, we utilize high-resolution imagery products from a rotary-wing UAV to characterize an eddy covariance footprint and scale up environmental sensor network observations to match the time-varying sampling area. Subsequently, in a surface and subsurface interaction study within a small watershed, we demonstrate the use of a fixed-wing UAV to characterize the spatial distribution of terrain attributes and vegetation conditions which serve as input to a distributed ecohydrologic model whose predictions compared well with an environmental sensor network. We also point to several challenges in performing ecohydrology with UAVs with the intent of promoting this new self-service (do-it-yourself) model for high-resolution image acquisition over many scales. We believe unmanned aerial vehicles can fundamentally change how ecohydrologic science is conducted and offer ways to merge remote sensing, environmental sensor networks and numerical models.

Key words: ecology; environmental sensor network; hydrology; remote sensing; robotics; scaling; unmanned aircraft systems.

Received 4 July 2014; revised 16 August 2014; accepted 23 August 2014; **published** 29 October 2014. Corresponding Editor: D. P. C. Peters.

† **E-mail:** vivoni@asu.edu

ECOHYDROLOGIC SCIENCE IN THE AGE OF DRONES

Ecohydrologic science has benefitted significantly from advances in remote sensing (e.g., Schmugge et al. 2002, Cohen and Goward 2004, Wood et al. 2011, Wang et al. 2012). Conventional remote sensing platforms, however, are limited to manned (piloted) aircraft and satellites (Hugenholtz et al. 2012), whose operation, product

definition, and data delivery are under the auspices of large organizations or agencies. The advent of unmanned aerial vehicles (UAVs), or unmanned aircraft systems, is poised to revolutionize the application of remote sensing to the earth and environmental sciences (e.g., Dunbabin and Marques 2012, Anderson and Gaston 2013). UAVs will offer the opportunity for individual scientists and small teams to obtain low-cost, repeat imagery at high resolutions (~1 cm to 1 m) tailored to the specific areas, products and delivery times of research interest (Rango et al. 2009, Rango and Laliberte 2010). While stemming from military developments in flight control, robotics, and miniaturized platforms and sensors, UAVs are now feasible for civilian applications due to the streamlining of image acquisition, processing and product delivery. This self-service model can fundamentally change how ecohydrologic science is conducted and the ways in which imagery is merged with environmental sensor networks and numerical models.

Several barriers are currently present to the broad-scale adoption of UAVs, or 'drones', as a common tool for ecohydrologic science. Foremost is the current regulatory framework in the United States and the associated public debates on safety and privacy (see Rango and Laliberte 2010, Hardin and Jensen 2011, Hugenholtz et al. 2012 for discussions), with other countries having more progressive approaches. In addition to delays in their broad use in U.S. airspace, a second barrier has been the lack of demonstrations on the utility of UAVs for ecological and hydrological applications. *Is it possible to advance ecohydrologic characterizations, process understanding, and predictive skills using remote sensing products from unmanned aerial vehicles?* Here, we demonstrate the operational flexibility of two types of UAVs that integrate four elements for autonomous data acquisition at low altitudes (~30–200 m): (1) a gasoline-powered aircraft with positional, velocity and attitude sensors, (2) an on-board computer for flight control and interfacing with sensors, (3) payloads for optical, thermal and multispectral image acquisition, and (4) a wireless network for sending flight instructions and receiving imagery. The overall goal is to translate the research-grade capabilities of small, autonomous vehicles into remotely-sensed imagery superior to those obtained from manned aircraft and satellite platforms in terms of spatial and temporal resolution and accuracy, but at lower costs and with greater operational versatility for the individual scientist and/or research team.

This article is aimed at introducing the utility of unmanned aerial vehicles within the data analysis and modeling workflows that are becoming common practice in the emerging field of ecohydrology, commonly defined as the interdisciplinary study of the interactions of water and ecosystems (e.g., Rodríguez-Iturbe 2000, Newman et al. 2006). We focus on UAV deployments over two study areas with long-term research efforts to illustrate how this emerging technology can provide novel insights in ecohydrologic studies at two scales—for land-atmosphere investigations at eddy covariance tower sites and for surface and subsurface interaction studies in small watersheds. In both cases, we use the UAV-derived products to interpret and extrapolate continuous observations from environmental sensor networks, which are considered to be a cornerstone of modern field investigations (Hart and Martinez 2006). We also use UAV-derived products as inputs into a distributed parameter model, the Triangulated Irregular Network (TIN)-based Real-time Integrated Basin Simulator (tRIBS, Ivanov et al. 2004), which is representative of modern modeling tools for ecohydrological applications (e.g., Tague and Band 2004, Niu et al. 2014). Since UAVs are primarily a new platform through which existing sensors can be rapidly deployed in a cost-effective manner, many of the advances in digital photogrammetry, Light Detection and Ranging (LiDAR) and multispectral data processing from manned aircraft and satellite observations can be readily transferred.

Multiple Unmanned Aerial Vehicles at Two Study Sites

A number of different unmanned aerial vehicle platforms currently exist with potential applications to ecohydrology (see Dunbabin and Marques 2012, Anderson and Gaston 2013). These platforms can generally be classified into two types, fixed- or rotary-wing UAVs, although

alternative methods using kites (McGarey and Saripalli 2013), tethered balloons (Johnson et al. 2014), and bird flight mimicry (Mackenzie 2012) are also in use. Recent studies have highlighted the scientific applications of UAVs in the disciplines of ecology (e.g., Laliberte and Rango 2011, Getzin et al. 2012, Dandois and Ellis 2013), geomorphology (e.g., Stefanik et al. 2011, d'Oleire-Oltmanns et al. 2012, Niethammer et al. 2012) and atmospheric science (e.g., Dias et al. 2012, Thomas et al. 2012, Reineman et al. 2013). Nevertheless, there has been a very limited use of UAVs in ecohydrology, with some examples related to mapping river morphology (Lejot et al. 2007), and assessing crop water status (Baluja et al. 2012).

Our efforts have concentrated on the deployment of two classes of UAVs (fixed- and rotary-wing) at rangeland sites in the southwestern United States: the Santa Rita Experimental Range (SRER) near Green Valley, Arizona, and the Jornada Experimental Range (JER) near Las Cruces, New Mexico. Fig. 1a depicts the two sites relative to their locations in the Sonoran and Chihuahuan Deserts, respectively. Both locations are representative of the process of woody plant encroachment, a long-term ecohydrological phenomenon that leads to the establishment of woody trees or shrubs in desert grasslands (e.g., Scholes and Archer 1997, Van Auken 2000). This can be readily seen in high-resolution image mosaics (Fig. 1b, c) depicting the distributions of trees, shrubs, grasses and bare soil patches, including the effect of ephemeral reaches on these patterns. In addition to their representative nature, each site was selected due to the existence of long-term precipitation and runoff records in two small watersheds (~1 ha or 0.01 km^2) in SRER (Polyakov et al. 2010) and one watershed (~5 ha or 0.05 km^2) in JER (Turnbull et al. 2013).

Fig. 2 presents the two UAV platforms deployed at the SRER and JER sites: the rotary-wing SR30 helicopter (Rotomotion LLC, Charleston, SC) and the fixed-wing BAT 3 airplane (MLB Company, Santa Clara, CA). After manual launching from a catapult (BAT 3) or vertical takeoff (SR30), each autonomous vehicle is controlled through a wireless network from a central location (canopy tent or trailer) from which flight information and adjustments are sent and rapid images retrieved (Rango et al. 2009, Lin and Saripalli 2012). Due to current Federal Aviation Administration (FAA) regulations, the autonomous operation requires an on-the-ground pilot who maintains line-of-sight with the UAV at all times (see discussion on operational rules in Rango and Laliberte 2010). Autonomous flight patterns from each platform are tailored to the size of the study area, the flight altitude and duration, and the desired ground resolution of the UAV-derived products. Table 1 compares the two UAV platforms, indicating the trade-offs that exist between flight altitude, duration and payload capacity. Data processing constraints, such as requirements for aerial image overlaps to ensure horizontal and vertical accuracy (e.g., Laliberte and Rango 2011, Fonstad et al. 2013), also play an important role. To protect equipment and ensure safety, landing is typically performed manually either to a landing pad (SR30) or on a dirt airstrip (BAT 3). Due to the rapid and low-cost UAV deployments and the experiences gained at each site, repeat flights have been carried out to capture seasonal variations in vegetation cover, with a focus on conditions prior to during and after the North American monsoon (Laliberte et al. 2011, Templeton et al. 2014).

The capacity to carry multiple payloads and trigger image acquisition simultaneously affords UAV platforms an advantage over other methods. Table 1 describes the current optical, multispectral and thermal sensors available on the fixed- and rotary-wing UAVs and estimates of the ground resolution (<0.5 m) obtained from typical altitudes. For each sensor type, we have developed workflows for image acquisition, orthorectification, and mosaicking using the global positioning system and inertial measurement unit (GPS/IMU) onboard each UAV (e.g., Laliberte and Rango 2011, Lin and Saripalli 2012). Fig. 1c illustrates the type of color image mosaics at 6 cm resolution obtained at JER from the BAT 3 platform, where over 30,000 images and 200 mosaics have been generated since 2006 (Rango et al., *in press*). Workflows also include a range of image processing techniques to extract features using object-based classification (Laliberte et al. 2012), to derive three-dimensional point clouds from image mosaics (Krishnan et al. 2012), and to calibrate multispectral images for

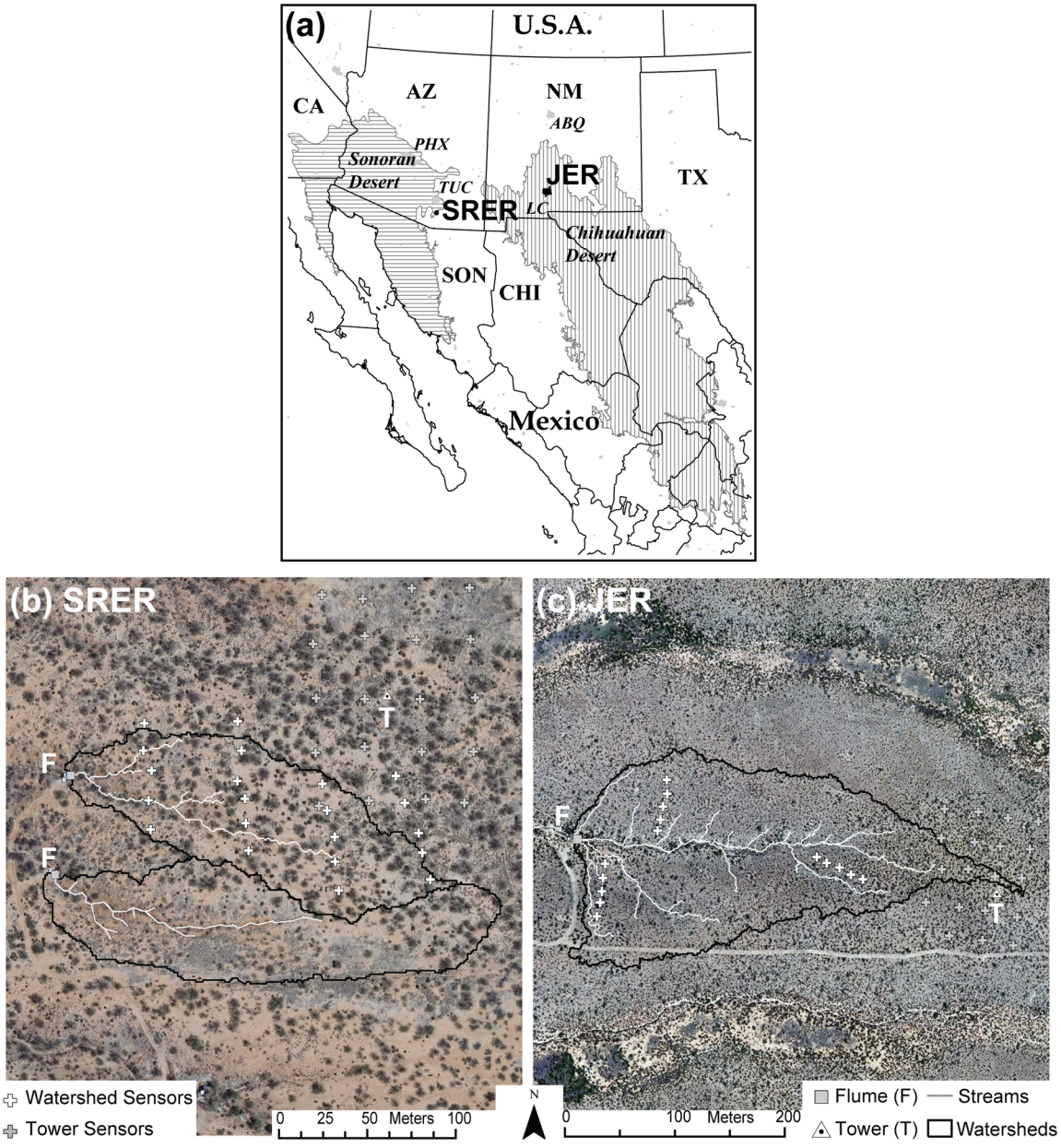

Fig. 1. (a) Location of the study watersheds relative to Sonoran and Chihuahuan Deserts (shaded regions) along the US and Mexico border. Color aerial photographs at SRER (b) and JER (c) with location of outlet flumes (F), eddy covariance towers (T) and soil sensor profiles in watersheds and around towers. High-resolution depictions of the watershed boundaries and stream networks were derived from 1 m digital elevation models (DEMs) obtained through a manned aircraft (b) and a fixed-wing unmanned aerial vehicle (c).

vegetation mapping (Laliberte et al. 2011). Image analyses from the multiple UAV classes have yielded a wealth of multi-temporal, high-resolution datasets that can be linked to ground surveys of terrain, vegetation or soil conditions (e.g., Anderson 2013, Pierini 2013, Templeton et al. 2014). Furthermore, the site characterizations possible with the UAV-derived products at different scales are useful for examining continuous ecohydrologic measurements or for con-

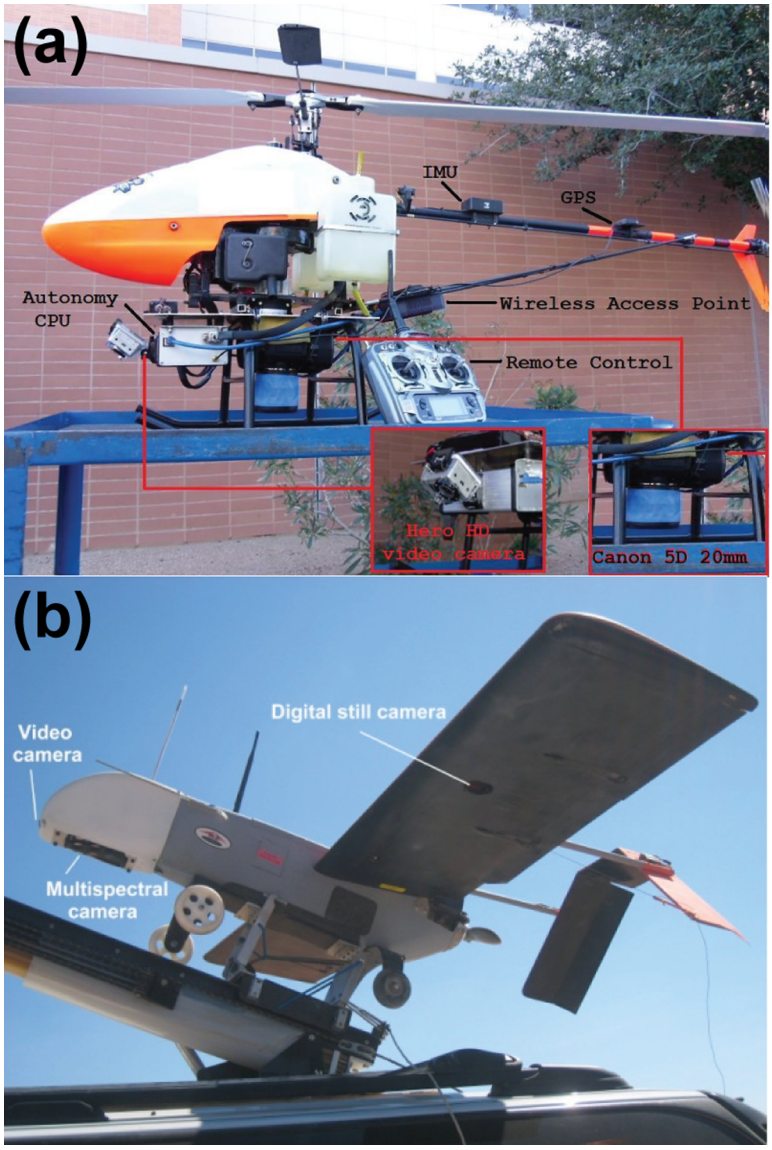

Fig. 2. Photographs of rotary-wing (a, deployed at SRER and JER) and fixed-wing (b, deployed at JER) UAV platforms, including sensor packages.

Table 1. UAV platform and sensor characteristics.

UAV platform characteristic	BAT 3	SR30
Owner and operator	USDA-ARS Jornada Experimental Range	Arizona State University
Gross weight	11 kg	16 kg
Typical and maximum flight altitudes	210 m and 3,048 m	30 m and 760 m
Flight speed range	62–110 km/hr	0–37 km/hr
Flight endurance or length	2 to 6 hours	1.5 hours
Payload weight	2 kg	4.5 kg
Sensors and approximate ground data resolution	Canon SD900 camera (0.06 m) Multispectral Tetracam (0.13 m) FLIR Thermal camera (0.28 m) Video camera	Canon EOS 5D camera (0.01 m) FLIR Thermal camera (0.04 m) Hero HD Video camera

ducting modeling activities, as discussed in the following.

Applications to Land-Atmosphere Interaction Studies

Anderson and Gaston (2013) suggest that unmanned aerial vehicles might be useful for characterizing the time-variable sampling footprints around eddy covariance (EC) sites. For areas with heterogeneous cover, this is particularly important given the differing sensible, latent and ground heat flux contributions from bare patches and different plant species (e.g., Detto et al. 2006, Vivoni et al. 2010). Fig. 3 presents an example of the utility of the rotary-wing UAV in a recent land-atmosphere interaction study conducted at the SRER, with an analogous effort at JER (Anderson 2013). We acquired images from low-altitude SR30 flights (~30 m), mosaicked the 5 cm images using the Structure from Motion (SfM, e.g., Turner et al. 2012) technique (Fig. 3a) and classified them based on the pixel values of the Red, Green and Blue (RGB) signature into three types (grass, tree and soil, Fig. 3b). The vegetation classification provides a means to aggregate the ground-based measurements of soil moisture and soil temperature obtained from a network of twenty sensor profiles established in the EC footprint. Thus, the UAV-derived vegetation map is a novel means to up-scale the land surface conditions sampled by the environmental sensor network within the daily sampling footprint of the EC site. We estimated the EC footprint using the model of Kormann and Meixner (2001) at the daily scale, aggregated this to the summer season in 2012 and displayed it as the 50% contribution contour line in Fig. 3. Note how twelve sensor profiles lie in the time-averaged EC footprint for this season, while others fall outside. The locations of daily peak flux contributions (stars in Fig. 3a) are typically clustered around the EC tower (T). A few sensor profiles were placed in a large grass area located 30 m north of the tower and contribute to the observed fluxes during days with northerly winds (Anderson 2013).

The high resolution afforded by the UAV-derived imagery opens the door for detailed spatial analyses to link the EC footprint (FP) to the environmental sensor network. Fig. 3b illustrates this by comparing the FP for September 13, 2012, shown as 3 m pixel percentage contributions, to the spatial distribution of daily-averaged soil moisture (SM). For this day, areas with larger contributions occur to the south, southeast and northwest of the tower and exhibit higher SM. A spatial average of soil moisture in the daily FP can be estimated by weighting those sensor profiles within specific patches using the vegetation percentages in the daily FP (Anderson 2013). Spatially-aggregated conditions in the FP can then be compared to latent, sensible and ground heat fluxes measured at the EC site (Vivoni et al. 2010). For example, Fig. 3c shows the observed latent heat flux at the EC tower and a nearby site (labeled 'alternate observation' and used to fill data gaps) during summer 2012. For September 13, 2012, the EC footprint and soil moisture spatial distributions (Fig. 3b) are linked to a period of high latent heat flux (~525 W/m^2) occurring a few days after a rainy period (~50 mm in two days). The observed latent heat flux is captured well for this day by a simulation using the tRIBS model (Pierini et al., *in press*) that accounts for the UAV-derived vegetation cover in the seasonal FP (67% grass, 23% tree, 10% soil). Furthermore, the model captures well the seasonal evolution of observed surface soil moisture in the environmental sensor network as well as conditions during the day of interest (Fig. 3d). Here, spatial averages and standard deviations are shown for 21 sensor profiles (including the EC site) weighted by the vegetation distribution in the seasonal FP.

The application of a rotary-wing UAV to a land-atmosphere interaction study at SRER showed the utility of the high-resolution imagery products for deriving a vegetation map used to scale up ground measurements and weight model simulations in an eddy covariance sampling footprint. Several challenges remain with respect to the use of UAVs at the space and time scales of eddy covariance measurements (see a broader discussion of challenges in Hardin and Jensen 2011). We based this example on a single flight in March 2011 prior to summer greening due to the North American monsoon (Forzieri et al. 2011). Repeat UAV flights coinciding with phenological stages would significantly improve the vegetation classification. This would allow for a time-variable weighting of the environmental sensor network and model outputs that

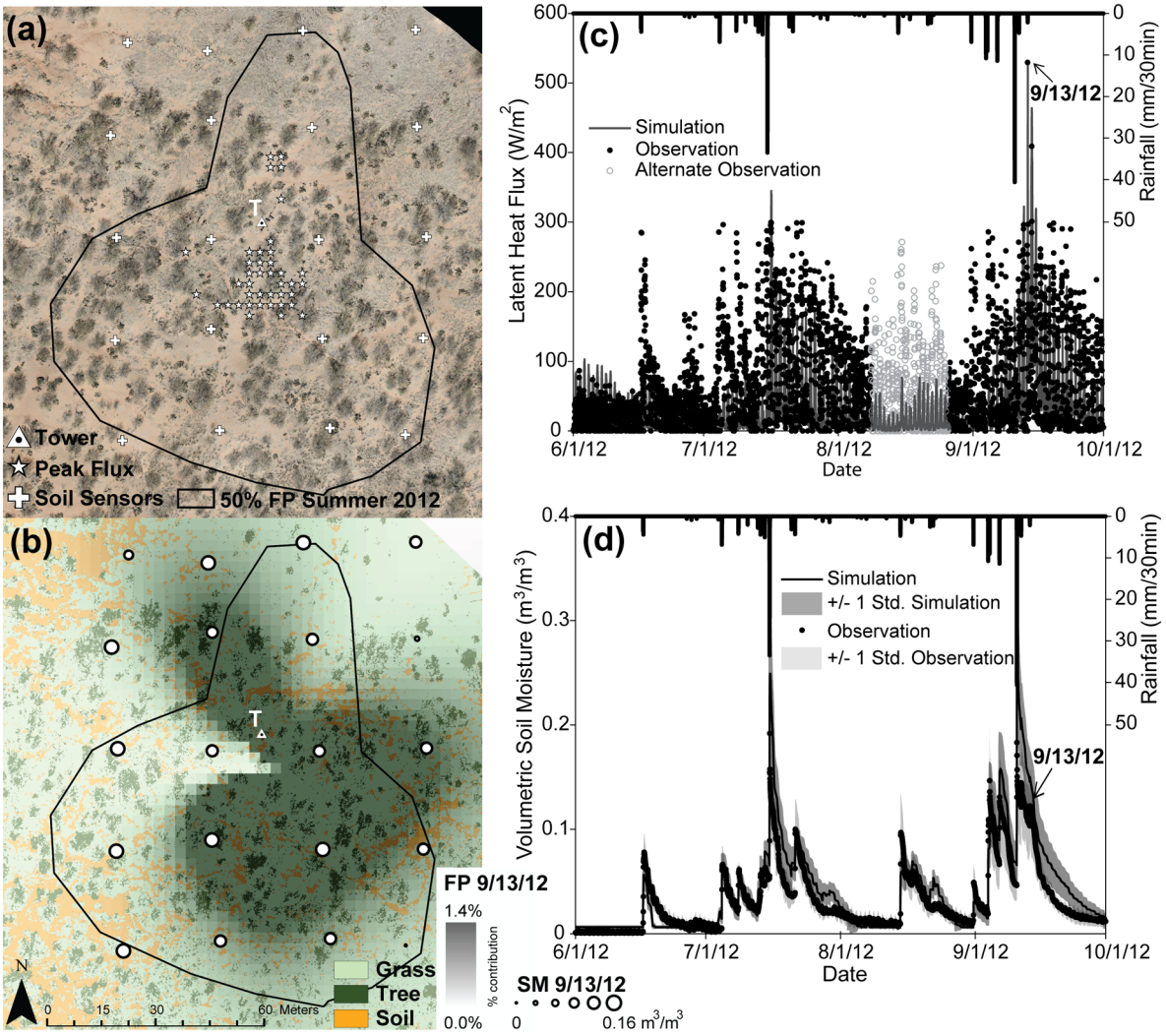

Fig. 3. Application of UAV products for land-atmosphere interaction studies. (a) 5 cm resolution RGB image from rotary-wing UAV near EC tower at SRER with twenty soil moisture and temperature sensor profiles (5, 15 and 30 cm depths). Also shown are the boundary of the EC footprint (FP) at 50% contribution for summer 2012 (July 1 to September 30) and locations of peak footprint contributions from individual days in that period. (b) 2 m resolution vegetation classes derived from the UAV RGB image in three categories (grass, tree and soil) along with the percent footprint contribution in 3 m resolution pixels for a single day (September 13, 2012). Also shown is the spatial distribution of measured volumetric soil moisture (SM) at 15 cm depth averaged for that day. (c) Comparison of simulated and observed latent heat flux at the EC site for summer 2012. Simulations account for UAV-derived vegetation cover in the FP (67% grass, 23% tree, 10% soil). Alternate observation during the period of instrument failure was obtained from a nearby (1 km distant) EC site. (d) Comparison of simulated and observed volumetric soil moisture (m^3/m^3) in top 10 cm for summer 2012. This is shown as spatial averages (solid lines) and spatial standard deviations (±1 std envelope) across 21 sensor profiles in the northern watershed (Fig. 1b) weighted according to the vegetation cover in the EC footprint.

account for the daily variability in the sampling footprint as well as less frequent variations (e.g., weekly to monthly, depending on UAV flight scheduling) in vegetation structure. Furthermore, multispectral imagery from a UAV over different time periods would allow a direct estimation of vegetation indices, such as the Normalized Difference Vegetation Index (NDVI), that are suited for characterizing vegetation type and phenology (e.g., Laliberte et al. 2011). Accounting for time-variations in vegetation can also provide a means to update model parameters, such as albedo, vegetation cover and canopy storage capacity (see Vivoni 2012*b*, Méndez-Barroso et al. 2014), which should improve the model agreement with latent heat flux observations during the seasonal evolution and add a time-variation to the spatial controls exerted by vegetation.

Applications to Surface and Subsurface Interaction Studies

Wood et al. (2011) suggest that hyperresolution modeling of surface and subsurface interactions requires observations on the order of tens of meters. Although it is more likely that satellite-based platforms will meet this need over large regions, UAVs provide finer resolution datasets (<1 m) useful for disaggregating coarser products. In addition, UAV-derived products can be used to parameterize and test ecohydrology models in ways analogous to the use of LiDAR data from manned aircraft (Mahmood and Vivoni 2011, Gutiérrez-Jurado and Vivoni 2013). Fig. 4 is an example of the utility of a fixed-wing UAV for a surface and subsurface study at the Tromble Weir (TW) watershed at JER, with an analogous effort occurring at SRER. We conducted low-altitude (~200 m) flights with the BAT 3 over the area about four times per year (2010–2013) to coincide with plant phenology stages (Templeton et al. 2014). For each flight, high-resolution (6 cm), overlapping RGB images were orthorectified using a set of ground control points and mosaicked to cover the TW watershed. Initially, the watershed boundary and stream network were known imprecisely based on a ground survey with a low accuracy GPS (see Rango et al., *in press*). Using an image mosaic from October 2010, we derived a 1 m 'bare earth' digital elevation model (DEM, Fig. 4a) and a 1 m canopy height model (CHM) from the three-dimensional point cloud and tested both products with a high-accuracy, differential GPS and plant height measurements at about 100 locations. We then conducted terrain processing of the DEM to derive maps of terrain slope, curvature, single-flow direction, upstream area and the stream network. Fig. 4a, c depict the watershed and sub-watersheds upstream of the outlet (Smith et al. 1981) and three internal flumes (Wainwright et al. 2002) as well as the stream network, which was verified using the differential GPS. Clearly, the UAV products provide novel insight into the terrain characteristics of the study site (see Templeton et al. 2014).

Laliberte et al. (2011) describes our efforts to produce and test a species-level vegetation classification based on a BAT 3 flight with a multispectral camera in May 2011. Comparisons of the 1 m resolution classification to ~1100 identified plants revealed an accuracy of 87%. Fig. 4b shows the spatial distributions of two grass and seven shrub species in addition to bare soil, the dominant cover. Table 2 defines the acronyms used in Fig. 4b and provides areal estimates of the species-specific cover within three areas: the watershed boundary, the 50% contribution footprint of an EC tower (Templeton et al. 2014), and the 50% footprint of a COsmic-ray Soil Moisture Observing System (COSMOS) sensor (e.g., Zreda et al. 2008, 2012). Some species vary in their cover percentages across the three domains due to preferential terrain locations. For example, the shrub *Parthenium incanum* (mariola) occurs more frequently in the watershed as it is located on mild slopes rather than the flatter surfaces near the EC site (see Rango et al., *in press*). Associated with these patterns are canopy height estimates which can quantify how plant size is linked to terrain positioning (as possible with LiDAR, see Forzieri et al. 2009, Gutiérrez-Jurado and Vivoni 2013), with typically taller shrubs in the upper flat surfaces and within the stream network. The UAV-derived vegetation classifications also reveal the varying role of bare soil patches in the watersheds at JER (~66%) and SRER (~25%), indicating how different the vegetation organization is within the two woody plant encroachment areas (Anderson 2013).

High-resolution terrain and vegetation products provide a detailed context to interpret

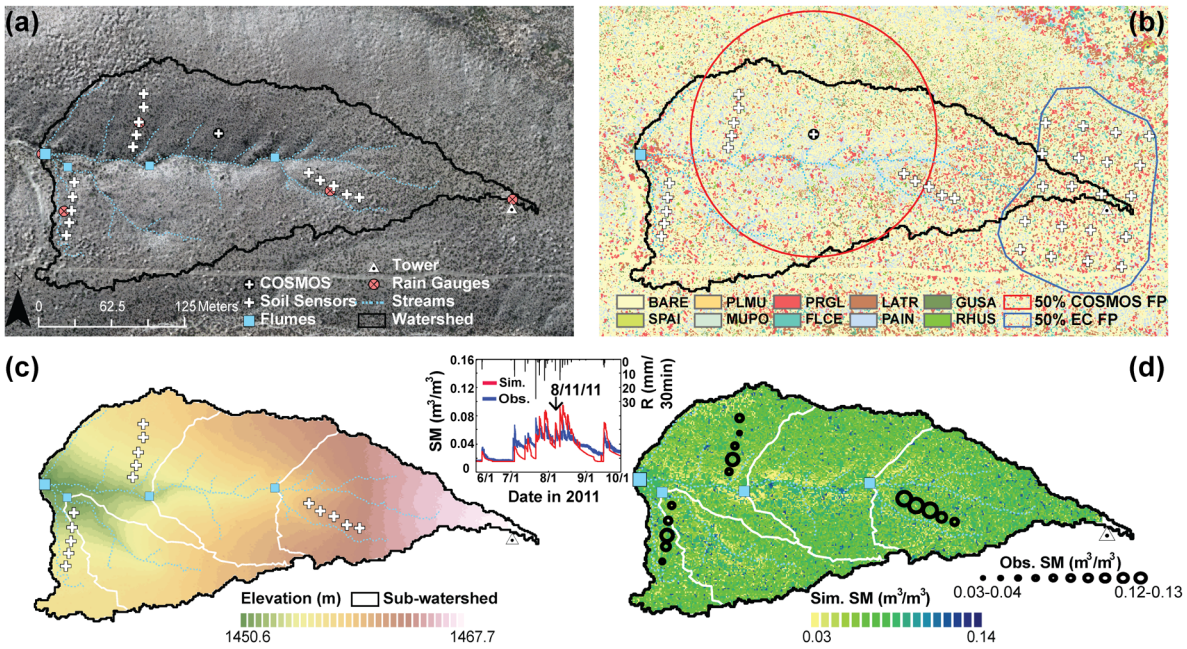

Fig. 4. Application of UAV products for surface and subsurface interaction studies. (a) 6 cm resolution RGB image from fixed-wing UAV superimposed on 1 m DEM near TW watershed at JER. Also shown are the locations of fifteen soil moisture and temperature sensor profiles (5, 15 and 30 cm depths), four runoff flumes, five rain gauges, an EC tower and a COSMOS sensor. (b) 1 m resolution species-level vegetation classification derived from the UAV RGB image (see Table 1 for vegetation types) along with the boundary of the EC FP at 50% contribution for summer 2012 and the boundary of the COSMOS footprint at 50% contribution. (c) Watershed elevations depicted in the tRIBS model consisting of 47,462 Voronoi polygons (resampled from 1 m DEM) and the boundaries of sub-watersheds upstream of internal flumes. (d) Comparison of simulated and observed daily volumetric soil moisture (SM, m^3/m^3) averaged over the top 40 cm in the watershed domain (color bar) and at sensor profile locations (graduated symbols) for August 11, 2011. Note the lower SM in bare areas along the northern banks of the main channel and higher SM in shrubs along and within the channels (b). A progressive wetting is also seen with closer proximity to the channel in both products. Inset compares simulated (red) and observed (blue) SM in the top 40 cm from June 1 to September 30, 2011, after averaging over the basin from all Voronoi polygons or using an aspect-elevation weighting of the sensor locations.

Table 2. Vegetation and bare soil classification in percentage of area for the TW watershed (46,700 m^2), EC footprint at 50% contribution (17,500 m^2) and COSMOS footprint at 50% contribution (34,600 m^2), as shown in Fig. 4b. ID refers to the abbreviation used in Fig. 4b.

Classification	ID	Watershed coverage (%)	EC footprint coverage (%)	COSMOS footprint coverage (%)
Bare soil	BARE	65.95	67.14	67.00
Parthenium incanum (mariola)	PAIN	11.94	3.84	6.20
Prosopis glandulosa (mesquite)	PRGL	6.47	8.92	8.30
Larrea tridentata (creosotebush)	LATR	5.82	7.79	7.21
Muhlenbergia porteri (bush muhly)	MUPO	2.89	4.62	4.17
Flourensia cernua (tarbush)	FLCE	2.48	4.85	4.57
Gutierrezia sarothrae (snakeweed)	GUSA	1.82	1.46	1.34
Pleuraphis mutica (tobosa grass)	PLMU	1.4	0.53	0.69
Rhus sp. (sumac)	RHUS	1.15	0.52	0.55
Sporobolus airoides (alkali sacaton)	SPAI	0.04	0.1	0.00
No data	...	0.02	0.23	0.00

observations from the environmental sensor network and to conduct ecohydrologic simulations. We established networks to sample water and energy states and fluxes within the watershed (Fig. 4a) and within the EC sampling footprint (Fig. 4b), derived in an analogous fashion to SRER. Based on the rainfall, soil moisture and runoff measurements, Templeton et al. (2014) tested if closing the watershed water balance provided accurate daily evapotranspiration estimates as compared to EC observations. A better match was obtained when soil moisture data from the three transects was averaged to the watershed scale using the UAV-derived aspect and elevation fields as a weighting scheme. Similarly, we found that the percentage cover of bare soil derived from the UAV within the time-variable EC footprint helped explain observed day-to-day differences in evaporative fraction, defined as the ratio of latent heat flux to total turbulent fluxes (Anderson 2013). Both terrain and vegetation products serve as spatially-distributed input to the tRIBS model applied to the TW watershed and as a means to upscale the sensor observations. Fig. 4c shows the high-resolution TIN (equivalent cell size of ~1 m for 47,462 Voronoi polygons) derived from the DEM along with the watershed boundary and stream network using the methods of Vivoni et al. (2004). Terrain attributes and vegetation types derived from the UAV products are captured explicitly in the Voronoi polygons. For example, the model domain incorporates higher slope areas near channel banks (Templeton et al. 2014) and the important connectivity between bare soil patches in areas with woody plant encroachment (e.g., Mueller et al. 2007, Okin et al. 2009). Effects of landscape characteristics are apparent in the surface and subsurface interactions simulated by the model. For example, Fig. 4d presents the observed and simulated depth-averaged SM for a single day (August 11, 2011). The model captures well the relatively high soil moisture occurring during this day when averaged over the basin (~0.07 m^3/m^3), as compared to observations that are aggregated using an aspect-elevation weighting scheme (Fig. 4d, inset), with adequate performance throughout the summer. Spatial patterns in soil moisture for August 11, 2011, show a progressive wetting toward the stream network in the model and observations, an indication of important lateral fluxes within hillslopes, as well as the controls of landscape features on soil moisture (e.g., drier areas along steep channel banks).

The high-resolution application of UAV products in the spatially-distributed model and the comparisons to the detailed environmental sensor network demonstrate the potential for exploring the link between spatial patterns and processes at the watershed scale (Vivoni 2012*a*). Several challenges remain in the application of UAVs to surface and subsurface interaction studies at the scales of interest to ecohydrology. We conducted our model-data intercomparisons in a relatively small (~5 ha) watershed that is not amenable to coarse (10–100 m) satellite-based observations to characterize, for example, land surface temperature or greenness patterns on a daily scale (e.g., Vivoni 2012*b*, Xiang et al. 2014). To do so would necessitate multiple flights from the same UAV (or multiple UAVs with similar sensors) over much larger regions at nearly the same time. If coordinated with satellite overpass times, the spatial variability of land surface states within satellite footprints could be quantified, in an analogous fashion to field campaigns with manned aircraft (e.g., Famiglietti et al. 1999, Mascaro et al. 2011), but at higher resolutions, reduced costs and lower logistical efforts. Furthermore, characterizing land surface temperature through thermal sensors, vegetation indices using a multispectral camera or possibly an index of soil wetness through their combination (e.g., Moran et al. 1994, Gillies et al. 1997) on board UAV platforms would provide much needed datasets to test the spatial predictions of ecohydrologic models. Clearly, the larger simulation regions would require using the parallel computing capabilities of spatially-explicit models (e.g., Vivoni et al. 2011, Wood et al. 2011) to conduct long-term simulations, ensemble forecasts or assessments of modeling uncertainty. In addition, UAVs and their derived products might help address an important uncertainty source, namely the spatial distribution of soil characteristics at scales comparable to terrain and vegetation patterns.

Future Directions

The advent of unmanned aerial vehicles as new platforms for remote sensing in the earth

and environmental sciences is part of the ever-increasing sophistication in technology available to individual scientists and small research teams. Coupled with environmental sensor networks, satellite-based remote sensing, and high-performance numerical modeling, ecohydrology and its allied fields are entering into an unprecedented period of data and model output availability, a new age of information to be assessed, classified and synthesized to monitor changes, advance process understanding and improve predictions in light of these changes (see, for example, Hampton et al. 2013). Empowered with the tailored products from UAVs in a self-service (do-it-yourself) approach, investigators could accurately track rapid landscape transformations, such as drought-induced plant mortality, invasive species, post-fire recovery or urbanization, in a spatially-explicit manner that can be integrated with more detailed monitoring at long-term sites such as the Long-term Ecological Research Network (LTER) or National Ecological Observing Network (NEON). Furthermore, *ecohydrology with UAVs* opens up new opportunities to approach the spatiotemporal resolutions required to understand the details of and adequately represent ecohydrologic systems faithfully in numerical models. How the ecohydrologic community deals with high-resolution imagery that approximates the actual scales of field observations and the scales of validity of model equations will dictate, to a large measure, our success in advancing the discipline and increasing our impact to society.

Acknowledgments

We thank funding from the U.S. Army Research Office (56059-EV-PCS) and the Jornada Long-Term Ecological Research project (NSF Grant DEB-1235828). We appreciate the support provided by the Jornada Experimental Range (J. Anderson, A. Slaughter, J. Lenz, D. Thatcher, C. Winters, P. Gronemeyer, C. Maxwell), USDA-ARS (D. P. C. Peters, K. Havstad, R. L. Scott, M. A. Nearing) and the Santa Rita Experimental Range (M. P. McClaran, M. Heitlinger). The efforts of Ryan C. Templeton, Brance Hudzietz and Yucong Lin are also appreciated.

Literature Cited

Anderson, C. A. 2013. Assessing land-atmosphere interactions through distributed footprint sampling at two eddy covariance towers in semiarid ecosystems of the southwestern U.S. Thesis. Arizona State University, Phoenix, Arizona, USA.

Anderson, K., and K. J. Gaston. 2013. Lightweight unmanned aerial vehicles will revolutionize spatial ecology. Frontiers in Ecology and the Environment 11:138–146.

Baluja, J., M. P. Diago, P. Balda, R. Zorer, F. Meggio, F. Morales, and J. Tardaguila. 2012. Assessment of vineyard water status variability by thermal and multispectral imagery using an unmanned aerial vehicle (UAV). Irrigation Science 30:511–512.

Cohen, W. B., and S. N. Goward. 2004. Landsat's role in ecological applications of remote sensing. BioScience 54:535–545.

Dandois, J. P., and E. C. Ellis. 2013. High spatial resolution three-dimensional mapping of vegetation spectral dynamics using computer vision. Remote Sensing of Environment 136:259–276.

Detto, M., N. Montaldo, J. D. Albertson, M. Mancini, and G. Katul. 2006. Soil moisture and vegetation controls on evapotranspiration in a heterogeneous Mediterranean ecosystem on Sardinia, Italy. Water Resources Research 42:W08419.

Dias, N. L., J. E. Goncalves, L. S. Freire, T. Hasegawa, and A. L. Malheiros. 2012. Obtaining potential virtual temperature profiles, entrainment fluxes and spectra from mini unmanned aerial vehicle data. Boundary-Layer Meteorology 145:93–111.

d'Oleire-Oltmanns, S., I. Marzolff, K. D. Peter, and J. B. Ries. 2012. Unmanned aerial vehicle (UAV) for monitoring soil erosion in Morocco. Remote Sensing 4:3390–3416.

Dunbabin, M., and L. Marques. 2012. Robotics for environmental monitoring. IEEE Robotics & Automation Magazine 3:24–39.

Famiglietti, J. S., J. A. Devereaux, C. Laymon, T. Tsegaye, P. R. Houser, T. J. Jackson, S. T. Graham, M. Rodell, and P. J. van Oevelen. 1999. Ground-based investigation of soil moisture variability within remote sensing footprints during the Southern Great Plains 1997 (SGP97) Hydrology Experiment. Water Resources Research 35(6):1839–1851.

Fonstad, M. A., J. T. Dietrich, B. C. Courville, J. L. Jensen, and P. E. Carbonneau. 2013. Topographic structure from motion: a new development in photogrammetric measurement. Earth Surface Processes and Landforms 38(4):421–430.

Forzieri, G., F. Castelli, and E. R. Vivoni. 2011. Vegetation dynamics within the North American monsoon region. Journal of Climate 24(6):1763–1783.

Forzieri, G., L. Guarneri, E. R. Vivoni, F. Castelli, and F. Preti. 2009. Multiple attribute decision making for individual tree detection using high-resolution laser scanning. Forest Ecology and Management 258:2501–2510.

Getzin, S., K. Wiegand, and I. Schoning. 2012. Assessing biodiversity in forests using very high resolution images and unmanned aerial vehicles. Methods in Ecology and Evolution 3:397–404.

Gillies, R. R., T. N. Carlson, J. Cui, W. P. Kustas, and S. Humes. 1997. A verification of the 'triangle' method for obtaining surface soil water content and energy fluxes from remote measurements of the Normalized Difference Vegetation Index (NDVI) and surface radiant temperature. International Journal of Remote Sensing 18(5):3145–3166.

Gutiérrez-Jurado, H. A., and E. R. Vivoni. 2013. Ecogeomorphic expressions of an aspect-controlled semiarid basin: II. Topographic and vegetation controls on solar irradiance. Ecohydrology 6:24–37.

Hampton, S. E., C. A. Strasser, J. J. Tewksbury, W. K. Gram, A. E. Budden, A. L. Batcheller, C. S. Duke, and J. H. Porter. 2013. Big data and the future of ecology. Frontiers of Ecology and the Environment 11:156–162.

Hardin, P. J., and R. R. Jensen. 2011. Small-scale unmanned aerial vehicles in environmental remote sensing: Challenges and opportunities. GIScience & Remote Sensing 48:99–111.

Hart, J. K., and K. Martinez. 2006. Environmental sensor networks: A revolution in the earth system science? Earth-Science Reviews 78:177–191.

Hugenholtz, C. H., B. J. Moorman, K. Riddell, and K. Whitehead. 2012. Small unmanned aircraft systems for remote sensing and earth science research. EOS, Transactions of the American Geophysical Union 93(25):236.

Ivanov, V. Y., E. R. Vivoni, R. L. Bras, and D. Entekhabi. 2004. Catchment hydrologic response with a fully-distributed triangulated irregular network model. Water Resources Research 40:W11102.

Johnson, K., E. Nissen, S. Saripalli, J. R. Arrowsmith, P. McGarey, K. Scharer, P. Williams, and K. Blisniuk. 2014. Rapid mapping of ultrafine fault zone topography with structure from motion. Geosphere 10:969–986.

Kormann, R., and F. X. Meixner. 2001. An analytical footprint model for non-neutral stratification. Boundary Layer Meteorology 99:207–224.

Krishnan, A. K., S. Saripalli, E. Nissen, and J. R. Arrowsmith. 2012. 3D change detection using low cost aerial imagery. IEEE International Symposium on Safety, Security and Rescue Robotics 1–6.

Laliberte, A. S., D. M. Browning, and A. Rango. 2012. A comparison of three feature selection methods for object-based classification of sub-decimeter resolution UltraCam-L imagery. International Journal of Applied Earth Observation and Geoinformation 15:70–78.

Laliberte, A. S., M. A. Goforth, C. M. Steele, and A. Rango. 2011. Multispectral remote sensing from unmanned aircraft: Image processing workflows and applications for rangeland environments. Remote Sensing 3(11):2529–2551.

Laliberte, A. S., and A. Rango. 2011. Image processing and classification procedures for analysis of sub-decimeter imagery acquired with an unmanned aircraft over arid rangelands. GIScience & Remote Sensing 48:4–23.

Lejot, J., C. Delacourt, H. Piegay, T. Fournier, M.-L. Tremelo, and P. Allemand. 2007. Very high spatial resolution imagery for channel bathymetry and topography from an unmanned mapping controlled platform. Earth Surface Processes and Landforms 32:1705–1725.

Lin, Y. C., and S. Saripalli. 2012. Road detection and tracking from aerial desert imagery. Journal of Intelligent and Robotic Systems 65(1-4):345–359.

Mackenzie, D. 2012. A flapping of wings. Science 335:1430–1433.

Mahmood, T. H., and E. R. Vivoni. 2011. A climate-induced threshold in hydrologic response in a semiarid ponderosa pine hillslope. Water Resources Research 47:W09529.

Mascaro, G., E. R. Vivoni, and R. Deidda. 2011. Soil moisture downscaling across climate regimes and its emergent properties. Journal of Geophysical Research: Atmospheres 116:D22114.

McGarey, P., and S. Saripalli. 2013. Autokite: Experimental use of a low cost autonomous kite plane for aerial photography and reconnaissance. International Conference on Unmanned Aircraft Systems 208–213.

Méndez-Barroso, L. A., E. R. Vivoni, A. Robles-Morua, G. Mascaro, E. A. Yépez, J. C. Rodríguez, C. J. Watts, J. Garatuza-Payan, and J. Saíz-Hernández. 2014. A modeling approach reveals differences in evapotranspiration and its partitioning in two semiarid ecosystems in northwest Mexico. Water Resources Research 50:3229–3252.

Moran, M. S., T. R. Clarke, Y. Inoue, and A. Vidal. 1994. Estimating crop water deficit using the relation between surface air temperature and spectral vegetation index. Remote Sensing of Environment 49(3):246–263.

Mueller, E. N., J. Wainwright, and A. J. Parsons. 2007. Impact of connectivity on the modeling of overland flow within semiarid shrubland environments. Water Resources Research 43:W09412.

Newman, B. D., B. P. Wilcox, S. Archer, D. D. Breshears, C. N. Dahm, C. J. Duffy, N. G. McDowell, F. M. Phillips, B. R. Scanlon, and E. R. Vivoni. 2006. The ecohydrology of arid and semiarid environments: A scientific vision. Water Resources Research 42:W06302.

Niethammer, U., M. R. James, S. Rothmund, J. Travelletti, and W. Joswig. 2012. UAV-based remote sensing of the Super Sauze landslide: evaluation and results. Engineering Geology 128:2–11.

Niu, G.-Y., C. Paniconi, P. A. Troch, R. L. Scott, M. Durcik, X. B. Zeng, T. Huxman, and D. C. Goodrich. 2014. An integrated modelling framework of catchment-scale ecohydrological processes: 1. Model description and tests over an energy-limited watershed. Ecohydrology 7:427–439.

Okin, G. S., A. J. Parsons, J. Wainwright, J. E. Herrick, B. T. Bestelmeyer, D. C. Peters, and E. L. Fredrickson. 2009. Do changes in connectivity explain desertification? BioScience 59(3):237–244.

Pierini, N. A. 2013. Exploring the ecohydrological impacts of woody plant encroachment in paired watersheds of the Sonoran Desert, Arizona. Thesis. Arizona State University, Phoenix, Arizona, USA.

Pierini, N. A., E. R. Vivoni, A. Robles-Morua, R. L. Scott, and M. A. Nearing. 2014. Using observations and a distributed hydrologic model to explore runoff threshold processes linked with mesquite encroachment in the Sonoran Desert. Water Resources Research 50, *in press*.

Polyakov, V. O., M. A. Nearing, M. H. Nichols, R. L. Scott, J. J. Stone, and M. P. McClaran. 2010. Long-term runoff and sediment yields from small semiarid watersheds in southern Arizona. Water Resources Research 46(9):W09512.

Rango, A., and A. Laliberte. 2010. Impact of flight regulations on effective use of unmanned aircraft systems for natural resources applications. Journal of Applied Remote Sensing 4:043539.

Rango, A., A. Laliberte, J. E. Herrick, C. Winters, K. Havstad, C. Steele, and D. M. Browning. 2009. Unmanned aerial vehicle-based remote sensing for rangeland assessment, monitoring and management. Journal of Applied Remote Sensing 3:033542.

Rango, A., E. R. Vivoni, C. A. Anderson, N. A. Pierini, A. P. Schreiner-McGraw, S. Saripalli, A. Slaughter, and A. S. Laliberte. 2014. Application of high resolution images from unmanned aircraft systems for watershed and rangeland science. *In* V. Lakshmi, editor. Remote sensing of the terrestrial water cycle. American Geophysical Union, Washington, D.C., USA. *in press*.

Reineman, B. D., L. Lenain, N. M. Statom, and W. K. Melville. 2013. Development and testing of instrumentation for UAV-based flux measurements within terrestrial and marine atmospheric boundary layers. Journal of Atmospheric and Oceanic Technology 30:1295–1319.

Rodríguez-Iturbe, I. 2000. Ecohydrology: A hydrologic perspective of climate-soil-vegetation dynamics. Water Resources Research 36:3–9.

Schmugge, T. J., W. P. Kustas, J. C. Ritchie, T. J. Jackson, and A. Rango. 2002. Remote sensing in hydrology. Advances in Water Resources 25(8-12):1367–1385.

Scholes, R. J., and S. R. Archer. 1997. Tree-grass interactions in savannas. Annual Review of Ecology and Systematics 28(1):517–544.

Smith, R. E., D. L. Chery, K. G. Renard, and W. R. Gwinn. 1981. Supercritical flow flumes for measuring sediment-laden flow. U.S. Department of Agriculture Technical Bulletin 1655.

Stefanik, K. V., J. C. Gassaway, K. Kochersberger, and A. L. Abbott. 2011. UAV-based stereo vision for rapid aerial terrain mapping. GIScience & Remote Sensing 48(1):24–49.

Tague, C., and L. Band. 2004. RHESSys: Regional hydro-ecologic simulation system: An object oriented approach to spatially distributed modeling of carbon, water and nutrient cycling. Earth Interactions 8:1–42.

Templeton, R. C., E. R. Vivoni, L. A. Méndez-Barroso, N. A. Pierini, C. A. Anderson, A. Rango, A. S. Laliberte, and R. L. Scott. 2014. High-resolution characterization of a semiarid watershed: Implications on evapotranspiration estimates. Journal of Hydrology 509:306–319.

Thomas, R. M., K. Lehmann, H. Nguyen, D. L. Jackson, D. Wolfe, and V. Ramanathan. 2012. Measurement of turbulent water vapor fluxes using a lightweight unmanned aerial vehicle system. Atmospheric Measurement Techniques 5:243–257.

Turnbull, L., A. J. Parsons, and J. Wainwright. 2013. Runoff responses to long-term rainfall variability in creosotebush-dominated shrubland. Journal of Arid Environments 91:88–94.

Turner, D., A. Lucieer, and C. Watson. 2012. An automated technique for generating georectified mosaics from ultra-high resolution Unmanned Aerial Vehicle (UAV) imagery, based on Structure from Motion (SfM) point clouds. Remote Sensing 4(5):1392–1410.

Van Auken, O. W. 2000. Shrub invasions of North American semiarid grasslands. Annual Reviews of Ecology and Systematics 31(1):197–215.

Vivoni, E. R. 2012*a*. Spatial patterns, processes and predictions in ecohydrology: Integrating technologies to meet the challenge. Ecohydrology 5:235–241.

Vivoni, E. R. 2012*b*. Diagnosing seasonal vegetation impacts on evapotranspiration and its partitioning at the catchment scale during SMEX04-NAME. Journal of Hydrometeorology 13:1631–1638.

Vivoni, E. R., V. Y. Ivanov, R. L. Bras, and D. Entekhabi. 2004. Generation of triangulated irregular networks based on hydrological similarity. Journal of Hydrologic Engineering 9:288–302.

Vivoni, E. R., G. Mascaro, S. Mniszewski, P. Fasel, E. P. Springer, V. Y. Ivanov, and R. L. Bras. 2011. Real-world hydrologic assessment of a fully-distributed hydrological model in a parallel computing environment. Journal of Hydrology 409:483–496.

Vivoni, E. R., C. J. Watts, J. C. Rodríguez, J. Garatuza-Payán, L. A. Méndez-Barroso, and J. A. Saiz-Hernandez. 2010. Improved land-atmosphere rela-

tions through distributed footprint measurements in a subtropical scrubland during the North American monsoon. Journal of Arid Environments 74:579–584.

Wainwright, J., A. J. Parsons, W. H. Schlesinger, and A. D. Abrahams. 2002. Hydrology-vegetation interactions in areas of discontinuous flow on a semiarid bajada, southern New Mexico. Journal of Arid Environments 51:319–338.

Wang, L., P. D'Odorico, J. P. Evans, D. J. Eldridge, M. F. McCabe, K. K. Caylor, and E. G. King. 2012. Dryland ecohydrology and climate change: Critical issues and technical advances. Hydrology and Earth System Sciences 16:2585–2603.

Wood, E. F., et al. 2011. Hyperresolution global land surface modeling: Meeting a grand challenge for monitoring Earth's terrestrial water. Water Resources Research 47:W05301.

Xiang, T. T., E. R. Vivoni, and D. J. Gochis. 2014. Seasonal evolution of ecohydrological controls on land surface temperature over complex terrain. Water Resources Research 50:3852–3874.

Zreda, M., D. Desilets, T. P. A. Ferre, and R. L. Scott. 2008. Measuring soil moisture content non-invasively at intermediate scales using cosmic-ray neutrons. Geophysical Research Letters 35:L21402.

Zreda, M., W. J. Shuttleworth, X. Zeng, C. Zweck, D. Desilets, T. Franz, and R. Rosolem. 2012. COSMOS: The Cosmic-ray Soil Moisture Observing System. Hydrology and Earth System Sciences 16:4079–4099.